Biomedical Research and Therapy 2024, 11(1):6125-6134

Open Access Full Text Article

Original Research

A mixture of secretions and extractions derived from antler stem cells heal open wounds in rats with a tendency to leave no scar

Phat Duc Huynh[1,*], Anh Le-Tram Cao[1], Thuan Minh Le[1], Sinh Truong Nguyen[2], Ngoc Bich Vu[1,2,*]

ABSTRACT

Introduction: Deer antlers are remarkable organs as they can regenerate seasonally and leave no scars. Antler-derived stem cell therapy applications are of increasing interest in food, beauty, and medicine. **Method**: Antler stem cells (ASCs) were isolated from antlers, and their expression of markers CD73, CD90, CD105, Nanog, and Oct4 was detected by PCR. Their capacity to differentiate into osteoblasts, chondrocytes, and adipocytes was assessed through culture in selection media. *In vitro* evaluations included wound healing and angiogenic effects using scratch and tube formation assay, respectively. For *in vivo* assessment, a rat skin defect model was established surgically, and ASC mixtures were applied to the defective skin at a dose of 100μg/100μl. Treatment effects were also evaluated through histological analysis, immunohistochemical staining, and the expression of genes involved in wound healing (including TGF-B1, TGF-B3, TIMP1, Col1, Col3, MMP1, and MMP3) using qRT-PCR method. **Results**: The results indicated that ASCs exhibited fibroblast-like cell shapes and positively expressed specific stem cell markers (CD73, CD90, CD105, Nanog, Oct 4). ASCs demonstrated the capability to differentiate into osteoblasts, chondrocytes, and adipocytes. The products derived from ASCs significantly enhanced NIH-3T3 cell proliferation and stimulated angiogenesis in HUVEC on Matrigel compared to the control group. In the rat skin defect model, wounds treated with the ASC mixture were quicker to heal, starting from day 8, compared to the sham group (day 16). The wound area treated with the ASC mixture was significantly smaller than the control group on day 4 ($p < 0.05$). Furthermore, the gene expression ratio of TGF-β3/TGF-β1, MMP1/TIMP1, and MMP3/TIMP1 was significantly increased in the ASC group compared to the sham group ($p < 0.05$). **Conclusion**: This study highlights the robust wound-healing efficacy of ASC-derived products.

Key words: Antler stem cell, Damaged skin, Deer antler, Extraction, Stem cell, Secretions, Mesenchymal stem cell

[1]*Laboratory of Stem Cell Research and Application, University of Science, Vietnam National University Ho Chi Minh City, Viet Nam*

[2]*Stem Cell Institute, University of Science, Vietnam National University Ho Chi Minh City, Viet Nam*

Correspondence

Phat Duc Huynh, Laboratory of Stem Cell Research and Application, University of Science, Vietnam National University Ho Chi Minh City, Viet Nam

Email: hdphat@hcmus.edu.vn

Correspondence

Ngoc Bich Vu, Laboratory of Stem Cell Research and Application, University of Science, Vietnam National University Ho Chi Minh City, Viet Nam

Stem Cell Institute, University of Science, Vietnam National University Ho Chi Minh City, Viet Nam

Email: ngocvu@sci.edu.vn

History

- Received: Nov 01, 2023
- Accepted: Jan 24, 2024
- Published Online: Jan 31, 2024

DOI : 10.15419/bmrat.v11i1.855

INTRODUCTION

Deer antler velvet is a prized repository of medicinal herbs, extensively used to produce food, nutraceuticals, and functional foods. In various Asian cultures, antler velvet holds a significant place in traditional medicine due to its perceived multitude of beneficial biological properties, including robust antioxidant capacity, anti-arthritis and anti-osteoporosis benefits, and its potential for treating reproductive disorders in women [1,2].

Exclusive to male deer, antlers are regarded as secondary sexual characteristics that undergo rapid growth during the summer. In the natural environment, antler velvet demonstrates a unique capacity to regenerate without scarring or inducing fibrosis. The growing tip, a critical region dictating antler growth, harbors a substantial concentration of stem cells [1,3]. Researchers have long been able to isolate stem cells from antler velvet and culture them in the laboratory for extended periods [4]. Consequently, the characteristics of antler stem cells (ASCs) have been comprehensively investigated. ASCs express mesenchymal stem cell markers (including CD73, CD90, and CD105 [5]) as well as embryonic stem cells such as Oct4, Sox2, and Nanog [6].

In recent years, components derived from antler velvet, notably stem cells and extracts, have garnered significant interest in research and application [3]. Injecting ASCs into the tail veins of mice with damaged skin demonstrated substantial healing effects without detectable scarring in the lesion area [7]. Kmiecik *et al.* (2021) treated 20 patients with foot venous ulcers using ASC extract, significantly reducing the area/circumference of the lesion [?].

Yang *et al.* showcased the safety and efficacy of ASC extract in regenerating hair follicles: application to damaged mouse skin led to a significant increase in the number of hair follicles [8]. Notably, even using conditioned medium from ASCs in treating injured skin displayed positive regeneration outcomes

Cite this article : Huynh P D, Cao A L, Le T M, Nguyen S T, Vu N B. **A mixture of secretions and extractions derived from antler stem cells heal open wounds in rats with a tendency to leave no scar**. *Biomed. Res. Ther.* 2024; 11(1):6125-6134.

in rats [1,9]. These findings underscore the therapeutic efficacy of ASCs, demonstrating positive effects across diverse species. They suggest the potential for utilizing ASCs or ASC-derived secretions in xenotransplantation or other cosmetic applications.

In this study, ASCs were successfully isolated and characterized. The cells were verified to possess self-renewing capabilities and the capacity to differentiate into various cell lines. Products formulated with ASCs were assessed for their wound-healing properties both *in vitro* and in mouse models. The efficacy of these ASC-derived products was compared with a control group using DMEM/F12 media. The findings indicate that ASC secretions and extracts effectively treat lesions without scarring, showcasing significant potential in cell-free therapy.

MATERIALS AND METHODS

Antler stem cell isolation

Fresh velvet from sika deer, *Cervus nippon*, was obtained from farmers in Dong Nai, Vietnam. It was collected by cutting and refrigerated during transportation to the laboratory. Biopsies were performed approximately 0.5–1.0 cm from the velvet tip to target the growth zone. The velvet tissue was dissected by making two perpendicular lines at a quarter of the velvet's length, intersecting at the apical region. The collected tissue, comprising the velvet skin and dermis, was promptly placed into a sterile tube containing PBS supplemented with 5X penicillin/streptomycin. Tissue processing was carried out within 2 hours of the biopsy. The tissue samples were finely chopped into pieces measuring 0.5–1 mm^3 using a sterile scalpel. Subsequently, each piece was incubated in an MSCCult Animal medium (Regenmedlab, Ho Chi Minh City, Viet Nam). The cells were cultured in T25 flasks at 37°C with 5% CO_2.

Antler stem cell characterization

The expression of specific genes, including CD73, CD90, CD105, Oct4, and Nanog, was assessed using PCR after extracting total RNA with an Easy Blue Total RNA Extraction Kit. The PCR was performed using a Luna Universal One-Step RT-qPCR Kit and a real-time PCR device. Gel electrophoresis with ethidium bromide staining was utilized to visualize the target gene bands. The primers used for these evaluations are detailed in **Table 1**.

To assess the *in vitro* differentiation capability of ASCs, the researchers employed differentiation kits for osteogenesis, chondrogenesis, and adipogenesis. Specifically, the StemPro® Osteogenesis Differentiation Kit, StemPro® Chondrogenesis Differentiation Kit, and StemPro® Adipogenesis Differentiation Kit from Thermo Fisher Scientific were used. The differentiation induction was evaluated after 14–21 days using specific dyes: Alizarin Red S for osteoblasts, Alcian Blue for chondroblasts, and Oil Red O for adipocytes. These dyes help visualize and confirm the successful differentiation of ASCs into the respective cell lineages.

Since there were no specific evaluation criteria for ASCs, the study adopted criteria commonly used for human mesenchymal stem cells (hMSCs). This approach allows for a standardized assessment of ASCs based on widely accepted criteria for mesenchymal stem cells.

ASC mixture formulation

Secretions collection

From passage 3, 10^5 cells were cultured in a T25 flask with MSCCult Animal medium (Regenmedlab, Ho Chi Minh City, VN) until 80% confluence was reached. After washing with PBS, 2ml of DMEM/F12 medium (Gibco, USA) was added. ASCs were incubated for 48 hours, after which the conditioned medium (CM) was collected. The CM was centrifuged at 4000 g for 5 minutes to remove debris and other cells. The clarified CM was stored at –86°C until use.

Extraction collection

Cells from passage 3 were separated using Deattachment (Regenmedlab, Ho Chi Minh City, Viet Nam). After centrifugation to remove the supernatant, the cell fraction was reconstituted with 100 μl of DMEM/F12. ASCs were placed in a freezer at –86 °C for 30 minutes, and this procedure was repeated three times. The mixture was centrifuged at 4000g for 5 minutes, and the supernatant was collected and stored at –86°C.

Formulation of ASC mixture

The ASC mixture was formulated by combining 2ml of secretions with 100 μl extractions. The mixture underwent filtration using a 0.22 μm filter.

Protein Quantification

The total protein content of the mixture was quantified using the Bradford assay. Briefly, bovine serum albumin (BSA) (Sigma-Aldrich, USA) standards were prepared at concentrations of 0, 62.5, 125, 250, 500, and 1000 ug/mL in PBS (Regenmedlab, Ho Chi Minh City, Viet Nam). The ASC mixture sample (10 μl) and BSA standard were loaded into wells, and 200 μl

Table 1: Primer sequences for ASCs evaluation

No	Name	Primer	Sequence (5'-3')	Size (bp)	Accession Number
1	*GAPDH*	F	GGCGTGAACCACGAGAAGTATAA	119	XM_020902047.1
		R	CCCTCCACGATGCCAAACT		
2	*Nanog*	F	CACCCTCGACACGGACACT	283	XM_043882000.1
		R	CTGCTTGTAGCTGAGGTTCAA		
3	*Oct4a*	F	GTGGAGGAAGCTGACAACAA	352	XM_043907988.1
		R	AGCCTGGGGTACCAAAATG		
4	*CD73*	F	GGTCAAAGGTGCCTCCAATG	353	XM_043901016.1
		R	CAATCCCATTCTTCTCAACAGC		
5	*CD90*	F	TCAGCCTGACAGCCTGCCTG	334	XM_043901026.1
		R	CTTATGCCCCCACACCTGAC		
6	*CD105*	F	CTCTACCTCAGCCCGCACTTC	105	XM_020874951.1
		R	GATCTTGAGCTCAGGGATGGAT		

of Coomassie Blue G-250 dye (Sigma-Aldrich, USA) was added to each well. After removing air bubbles, the absorbance was measured at 595 nm using a DTX 880 machine (Beckman Coulter 880, USA).

Cell migration assay

The *in vitro* wound healing effect of the ASC mixture was evaluated using the Scratch test.

Human fibroblasts were provided by the Laboratory of Stem Cell Research and Application, University of Science, Viet Nam. We plated 10^5 fibroblasts into the well plate using a cell culture medium containing DMEM F12 + 10% FBS (Gibco, USA) (n = 3). Then, a 1ml pipette tip was used to create a wound along the well. Floating cells and cell debris were removed with PBS (Regenmedlab, Viet Nam). The experiment was randomly divided into two groups. In group 1, the ASC mixture was supplied at a concentration of 100ug/ml. In group 2 (the control group), DMEM/F12 supplied with 10% FBS was refreshed. Then, 2 ml of the media was added to the well (n = 3). Images were recorded for the first time and after 72 hours. The covered area was processed by ImageJ software.

Endothelial Cell Tube Formation Assay

Corning Matrigel Matrix (Corning, USA) was employed for *in vitro* angiogenesis, following the manufacturer's guidelines. Gibco^{TM} Human Umbilical Vein Endothelial Cells (HUVEC) (Thermo Fisher, USA) were cultured using EGM medium (Cell Applications, Inc, CA, USA) for proliferation. Matrigel (50 μl) was added to each well of a 96-well plate and allowed to polymerize for 30 minutes. Subsequently, 10^4 HUVEC cells were seeded into each well. The ASC mixture, containing 100 μg/ml of total protein, was added to three wells, while EGM medium served as a positive control and DMEM/F12 medium as a negative control. Images were captured after 6 hours using an inverted microscope (Zeiss, Germany).

Mouse model of skin damage

Six- to eight-week-old rats were procured from the Stem Cell Institute in Viet Nam, and all experimental procedures adhered to the guidelines and protocol of the Animal Experimental Ethics Committee of the Stem Cell Institute, University of Sciences, Viet Nam National University, Ho Chi Minh City (Number 230106/SCI-AEC). The dorsal region of the rats was shaved, and anesthesia was induced using 5 mg/kg Zoletil (Virbac, France) and 4 mg/kg xylazine (Vemedim, Viet Nam). A circular wound (8 mm diameter) was created on the back by marking and incising the skin in this designated area.

Subsequently, the rats were randomly assigned to three groups (n = 3 each). In the ASC mixture group, rats received a single injection of ASC mixture at a dose of 100 μg/100μl DMEM/F12. In the sham group, rats were injected with DMEM/F12 at an equivalent volume. The normal group consisted of mice that were not injured and were kept in identical conditions. Wound healing progress in each area was monitored over time, and all rats received consistent

acre conditions. After 16 days, the rats were euthanized, and the healed wound tissue area was collected using a scalpel.

Hematoxylin/Eosin (H&E) staining

The histological structures of each group were assessed on day 16 by collecting skin samples from the injured sites. These samples were fixed in 10% formaldehyde and subsequently embedded in paraffin. The paraffin-embedded sections were cut into slices of 3–5um thickness. The H&E staining protocol involved the following steps: the slices were immersed in a xylene solution for 5 minutes, followed by a xylene: alcohol solution (1:1 ratio) for another 5 minutes, 100% alcohol for 5 minutes, 90% alcohol for 5 minutes, 70% alcohol for 5 minutes, 50% alcohol for 5 minutes, and finally, double-distilled water for 2 minutes. Afterward, the slices were carefully blotted dry.

The staining process continued by adding a drop of hematoxylin to the slice. After 15 minutes, the slices were rinsed with double-distilled water to remove excess hematoxylin. Eosin was then applied to the slices for 30 seconds. Following this step, the slices were re-washed with double-distilled water. Finally, immersion oil was added to the slices and sealed with cover slips. Tissue histology was observed using a microscope (Zeiss, Germany).

qRT-PCR

The expression of specific genes associated with wound healing, including Col1, Col3, MMP1, MMP3, TIMP1, TGF-B1, and TGF-B3, was assessed on day 16. The housekeeping gene GADPH was utilized for normalizing these gene expressions. The Easy Blue Total RNA Extraction Kit (iNtRON Biotechnology, Korea) was employed to extract the total RNA from the skin samples according to the manufacturer's instructions. Quantitative RT-PCR was conducted using the Luna® Universal One-Step RT-qPCR Kit (Bio Labs, New England), following the manufacturer's protocol and utilizing a real-time PCR device (Eppendorf, Hamburg, Germany). The gene-specific primers are presented in **Table 2**. The expression levels of the target genes in the samples were compared to the non-treating group using the ratio calculated by the Livak method: $R = 2^{-\Delta\Delta Ct}$.

Statistical Analysis

The experimental data are presented as means + SD based on three independent treatments. Statistical analyses were conducted using two-tailed Student's t-tests and multiple T-tests using GraphPad Prism 8.0 software (Sorrento Valley, CA, USA). A statistically significant difference was considered when $p < 0.05$.

RESULTS

ASC isolation

After 4 days of primary culture, single cells were presented (**Figure 1** A) and exhibited adhesion to the flask surface (**Figure 1** B). The cellular morphology was fibroblast-like (**Figure 1** C).

Following a 14-day culture in an osteogenic medium, cells displayed a red coloration upon staining with Alizarin Red dye (**Figure 1** D). When subjected to a chondrogenic medium, the cells adopted a rounder shape. On day 14, the cells exhibited a blue coloration upon Alcian Blue staining, signifying the accumulation of peptidoglycan, a marker of successful chondrogenesis (**Figure 1** E). In the adipogenesis medium, the presence of fat droplets was observed. Staining with Oil Red revealed red-colored fat droplets, indicating successful adipose differentiation (**Figure 1** F). Immunophenotypic expression assessment demonstrated positive results for CD73, CD90, and CD105 markers of mesenchymal stem cells, as well as for Oct4a and Nanog, markers of pluripotent stem cells (**Figure 1** G). These outcomes confirm that the isolated alter cells exhibit typical characteristics of mesenchymal stem cells.

Cell migration *in vitro* assay

The initial wound area measured 0.458 ± 0.008 mm^2 in the control group (**Figure 2** A) and 0.489 ± 0.030 mm^2 in the ASC mixture group (**Figure 2** B). After 72 hours of culture, the wound area in the ASC group showed a statistically significant reduction compared to the pre-treatment measurement ($p < 0.05$). The wound area in the ASC mixture group (**Figure 2** D) reached 0.063 ± 0.021 mm^2, whereas in the control group (**Figure 2** C), it measured 0.306 ± 0.041 mm^2 (**Figure 2** E).

Angiogenesis *in vitro*

In the EGM medium, HUVEC exhibited notable tube formation (**Figure 3** A). Conversely, the DMEM/F12 treatment group displayed a lack of HUVEC adhesion to the Matrigel, resulting in distorted cell shapes. The cell appeared rounded, indicative of poor adhesion (**Figure 3** B). However, the treatment group did not show the characteristic tubular connection observed in the EGM medium.

Tube formation was observed in the case of the DMEM/F12 treatment combined with 100 μg/ml

Table 2: Primers were used to evaluate gene expression in rats

No	Gene name	Primers	Sequences (5'-3')	Product size (bp)	Accession Number
1	*Col1A2*	Forward	GGTGCCCCTGGAGAGAAT	158	NM_053356.2
		Reverse	GGACCAGCAGACCCAATG		
2	*Col3A1*	Forward	GTCCACGAGGTGACAAAGGT	189	NM_032085.1
		Reverse	CATCTTTTCCAGGAGGTCCA		
3	*TGF-β1*	Forward	ATACGCCTGAGTGGCTGTCT	153	NM_021578.2
		Reverse	TGGGACTGATCCCATTGATT		
4	*TGF-β3*	Forward	CTCTCTGTCCACTTGCACCA	185	XM_039111816.1
		Reverse	TGCATCTCTTCCAGCAACTCC		
5	*MMP1*	Forward	GCTTTGGCTTCCCTAGCAGTG	201	NM_001134530.1
		Reverse	TCGCCTTTTTGGAAAACATC		
6	*MMP3*	Forward	CCACCGAGCTATCCACTCAT	159	NM_031055.2
		Reverse	GTCCGGTTTCAGCATGTTTT		
7	*TMIP1*	Forward	CATGGAGAGCCTCTGTGGAT	210	XM_039099407.1
		Reverse	ATGGCTGAACAGGGAAACAC		
8	*GapDH*	Forward	CAACTCCCTCAAGATTGTCAGCAA	118	NM_001394060.2
		Reverse	GGCATGGACTGTGGTCATGA		

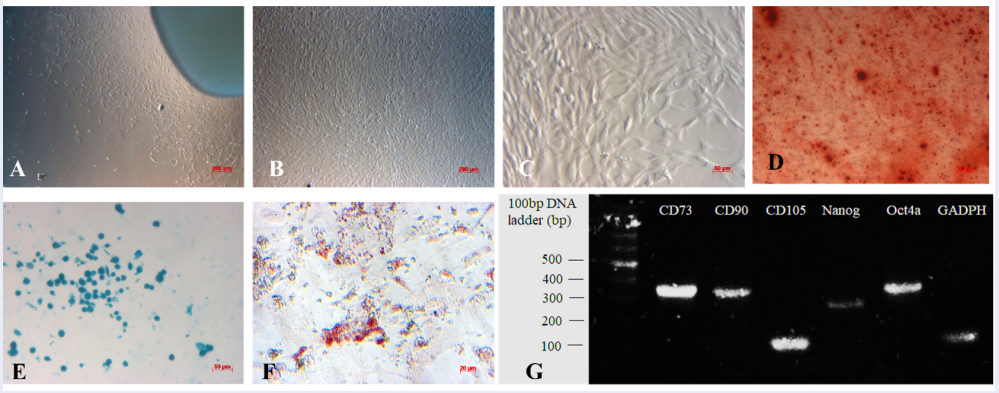

Figure 1: **ASC characterization**. Primary alter cell culture (**A**); secondary cell culture at 5X (**B**) and 20X (**C**); osteoblast differentiation-induced cells stained with Alizarin Red (**D**); chondroblast differentiation-induced cells stained with Alcian blue (**E**); adipogenesis differentiation-induced cells stained with Oil Red (**F**); PCR results showed that ASCs express genes CD73, CD90, CD105, Nanog, and Oct4a (**G**).

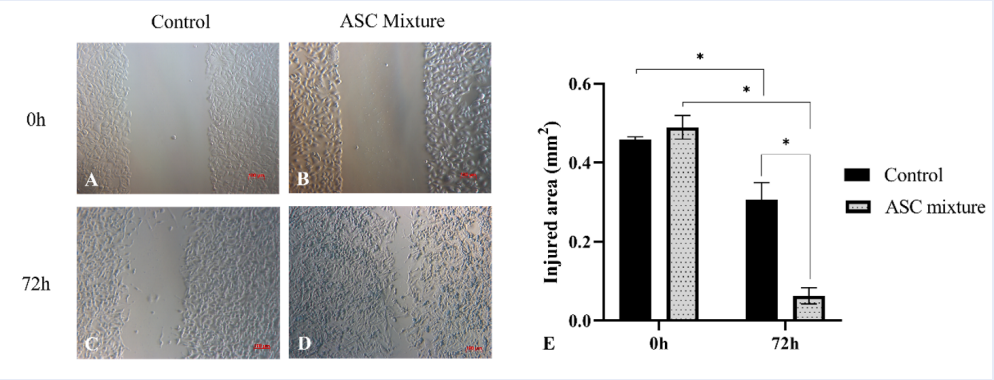

Figure 2: **ASC migration *in vitro***. *In vitro* wound shape of the control group (**A, C**) and ASC mixture group (**B, D**) at 0h (**A, B**) and 72h (**C, D**); comparison of the wound area before and after treatment (**E**).

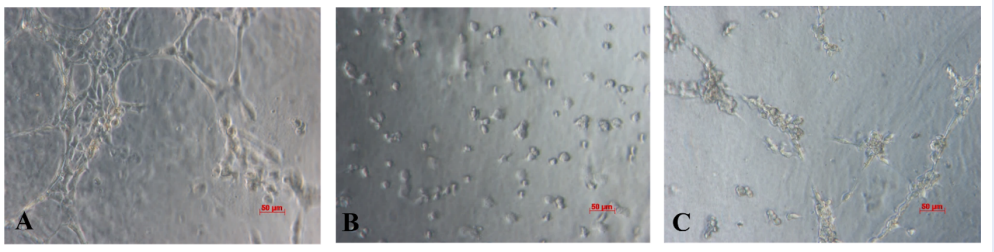

Figure 3: **Angiogenesis stimulation ability of ASC mixture *in vitro***. Tube formation of HUVECs when cultured in ECM medium (**A**), DMEM/F12 (**B**), and ASC mixture (**C**).

ASC mixture (**Figure 3** C). Nevertheless, this angiogenic response was less pronounced than the one observed with commercial media (**Figure 3** A).

Skin-injured rat treatment

On day 4 post-treatment, the wound area in the ASC mixture group exhibited accelerated healing compared to the sham group. Between days 8 and 12, the damaged area in the ASC mixture group rapidly diminished, while it took 16 days for the sham group to show a comparable reduction in the damaged area. However, noticeable scarring was observed in both groups until day 16 (**Figure 4** A).

ImageJ analysis showed that the wound area in the ASC mixture group was statistically significantly smaller (7.802 ± 3.120 mm^2) compared to the sham group (33.806 ± 6.689 mm^2) ($p < 0.05$) (**Figure 4** B). The ASC mixture group also showed positive and different effects than the sham group (**Figure 4** A).

H&E Staining

The normal skin tissue structure of the rat (**Figure 5** A, D, G) exhibits well-defined substructures (22.33 ± 5.033), including evenly distributed hair follicles (red arrows) and sebaceous glands (blue arrows) within the epidermis and mesoderm. Following a 16-day application of the ASC mixture, the rat skin structure was fully restored with a complete epidermal and mesodermal structure. Substructures such as hair follicles and sebaceous glands were present (15.67 ± 1.53), mirroring the tissue structure observed in the normal group (**Figure 5** B, E, G).

Conversely, in the DMEM/F12 group, the presence of substructures was significantly less (1.33 ± 1.53). Sebaceous glands and hair follicles were notably lacking (**Figure 5** C, F, G). These results indicate that treatment with the ASCs mixture enhances skin tissue recovery.

Gene expression

The gene expression ratio of MMP1/TIMP1 (0.009 ± 0.001; Fig. 6A), TGF3/TGF1 (1.580 ± 0.843; **Figure 6** B), and MMP3/TIMP1 (3.969 ± 0.924; **Figure 6** D) in the ASC mixture treatment group were all significantly higher than those in the DMEM/F12 control group (0.0002 ± 0.0001, 0.374 ± 0.220, $1.449 \pm$

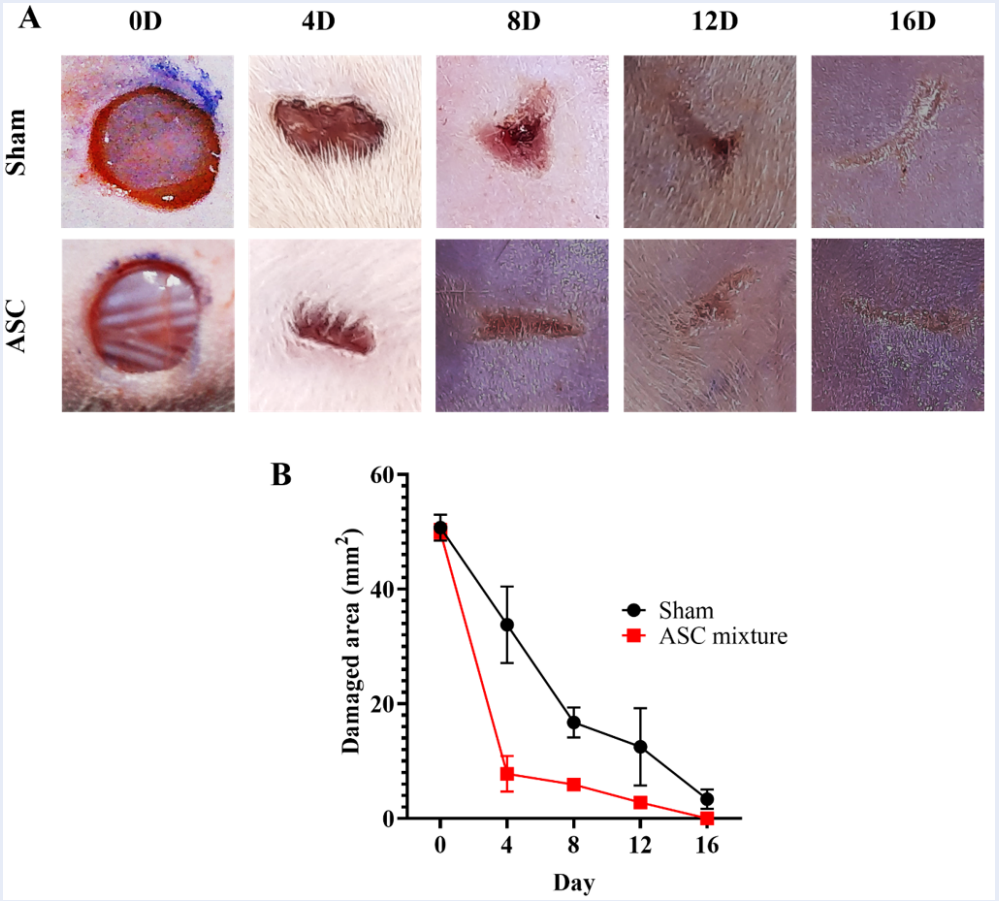

Figure 4: **The recovery of injured skin**. Morphology of skin at the damaged position from immediately after injury to 16 days post-treatment (**A**); the damaged area of the rat (**B**) (n = 3)

1.474, respectively) ($p < 0.05$). Meanwhile, the ratio of Col3/Col1 in the ASC treatment group tended to increase, although it did not reach statistical significance compared to the sham group (**Figure 6** C).

DISCUSSION

The complete regeneration of an organ is rare in higher animals, but antlers are an exception. Although ASCs have only been known for a decade, their potential is immense [10]. Attention toward products from mesenchymal stem cells, such as vesicles, exosomes, and growth factors, has increased exponentially in recent times [11].

The wound-healing effect of mesenchymal stem cells (MSCs) is established by proteins, lipids, growth factors, or nucleic acids that they secrete. These factors can act individually or in combination. Growth factors are of particular interest due to their clear mode of action on target cells. Many of the growth factors detected in MSCs are also present in ASCs. These factors play a crucial role in directing cell migration, proliferation, and angiogenesis [11].

In this study, the ASC product mixture was shown to stimulate wound healing and angiogenesis *in vitro*. In a rat skin injury model, the ASC product accelerated wound healing, and the healed wound structure closely resembled normal skin.

The impact on scar formation in vivo was assessed through gene expression analysis, including MMP1, TIMP1, MMP3, Col3, Col1, TGF3, and TGF1. The results indicated that the gene expression ratio of MMP1/TIMP1, MMP3/TIMP1, Col3/Col1, and TGF3/TGF1 was highest in the ASC mixture group. The collaboration between matrix metalloproteinases (MMPs) and tissue inhibitors of metalloproteinases (TIMP) has been shown to synergize in fetal wound healing [12]. Studies by Dang *et al.* and Rong *et al.* also support the finding that higher expression ratios between MMO and TIMP reduce wound scarring [1,13].

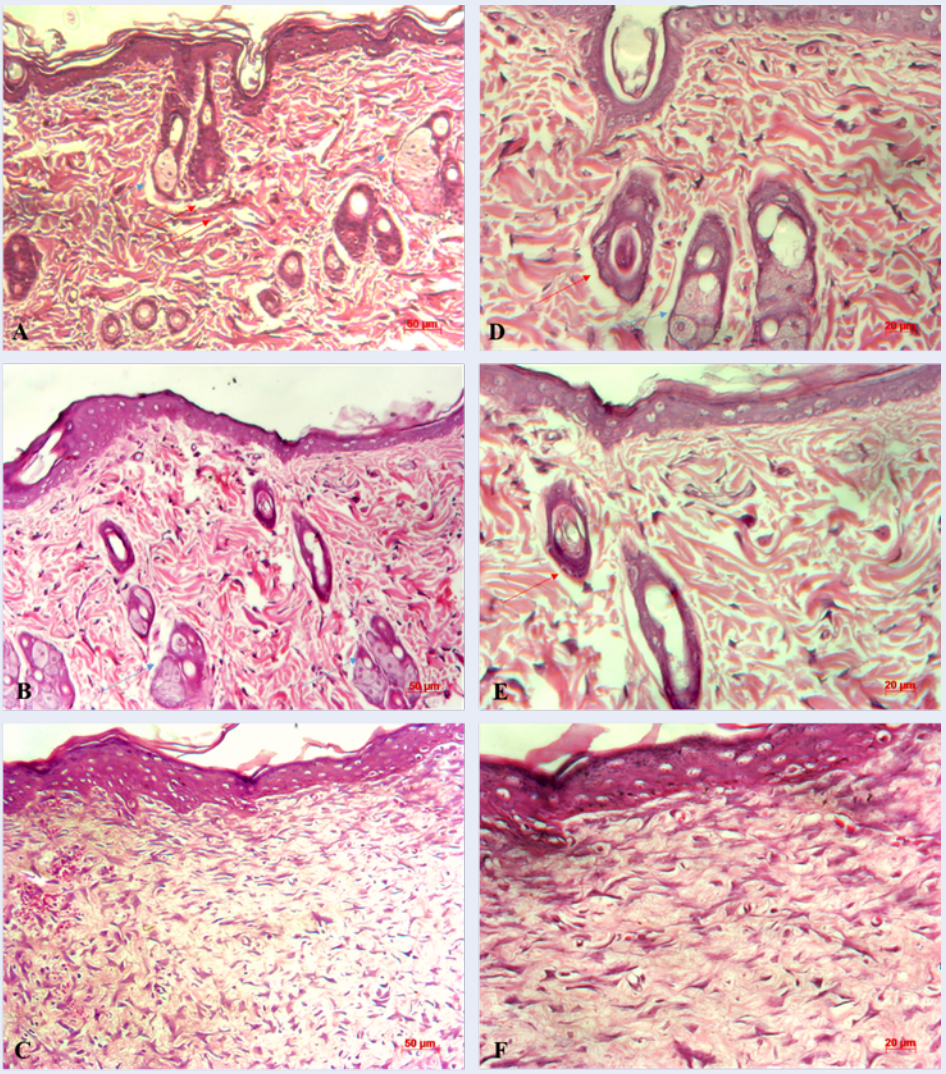

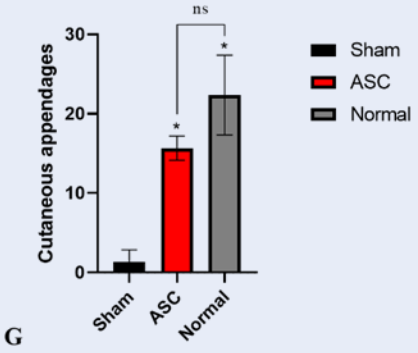

G

Figure 5: **H&E staining results of normal skin (A, D); wound areas of the group treated with the ASC mixture (B, E); and DMEM/F12 (sham) (C, F); G**. Number of cutaneous appendages (20x); (red arrows: hair follicles; blue arrows: sebaceous glands). (*$p < 0.01$) (**A, B, C** bar = 50 μm; **D, E, F** bar = 20 μm).

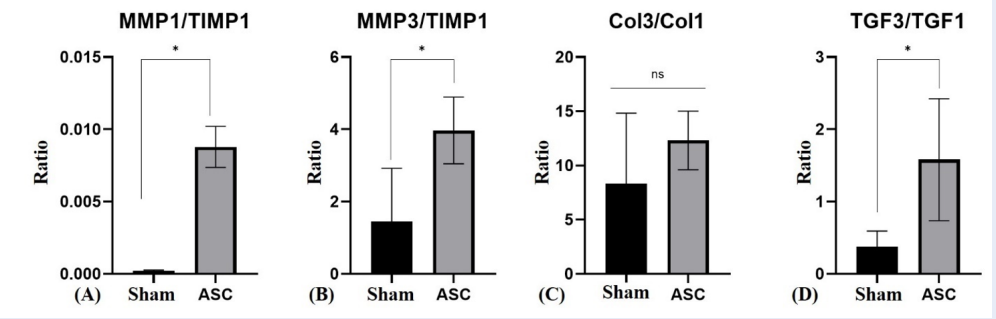

Figure 6: **Gene expression ratio of MMP1/TIMP1 (A), MMP3/TIMP1 (B), Col3/Col1 (C), and TGF3/TGF1 (D) of the mouse skin treated with various factors**. ($P < 0.05$)

Open wounds treated with the ASC mixture healed faster in this study, and the high MMP/TIMP ratio in this group resembled that of fetal wounds, leaving no scars. The active MMP group's activity facilitates the removal of the original bonds accumulated during wound repair, forming new structures that better mimic function. This study specifically focused on evaluating TIMP1, known for inhibiting the activity of most MMP families[14]. Another study also demonstrated that an increased ratio of MMP8/TIMP1 led to faster wound contraction and improved extracellular matrix layer reconstruction in open wounds, aligning with the results of this study[15].

The ratio of Col3/Col1 showed an increasing trend in both the DMEM/F12 (8.34 ± 6.48) and ASC (12.31 ± 2.7) groups, aligning with findings by Rong *et al.*[1] . Col3 is the initial and crucial collagen formed during wound healing, later replaced by Col1 during the repair process[16]. Col1 typically constitutes 85% of adult scarred areas, with the remaining 15% being Col3. Notably, our study observed a tendency towards an increased Col3/Col1 ratio in the ASC-treated group, resembling the expression pattern in fetal wounds that heal without scarring (reconstruction and rehabilitation)[1]. However, this difference was not statistically significant between the groups, which might be attributed to the young age of the mice (6–8 weeks old) since young animals are characterized by inherent resilience, which can influence collagen expression rates.

The ratio of TGF-β3/TGF-β1 in the ASCs mixture treatment group was higher than in the DMEM/F12 groups. The TGF-β family comprises proteins with diverse roles in various pathways. Specifically, TGF-β3 is more expressed in fetal wounds associated with good regeneration and no scarring, while TGF-β1 exhibits reduced expression in such wounds[17]. Krummel's study found that high levels of TGF-β1 supplementation induced fibrosis even in fetal wounds[18]. Our results underscore the positive impact of ASC mixture treatment on wounds compared to the DMEM/F12 group.

This study contributes valuable evidence to the unexpected effects of products derived from ASCs. While using hMSCs is common in treating various diseases, with mostly positive outcomes (https://clinicaltrials.gov/, keyword: mesenchymal stem cell), the continuous search for new therapies with enhanced efficacy, safety, and cost-effectiveness remains crucial. ASCs and their products demonstrate promising features in various applications, offering potential in medical therapies.

CONCLUSION

This study demonstrated the proliferative, migratory, and angiogenic effects of ASCs *in vitro*. In the mouse model of skin lesions, ASC extract and secretions exhibited superior results compared to the DMEM/F12 group. Notably, the healing trend associated with ASC-derived products suggests the potential to minimize scarring and maximize the restoration of the damaged area to resemble undamaged skin.

ABBREVIATIONS

ASC: Antler stem cell, **CD**: Cluster of differentiation, **Col**: Collagen, **FBS**: Fetal Bovine Serum, **hMSC**: Human mesenchymal stem cell, **HUVEC**: Human umbilical vein endothelial cells, **MMP**: Matrix metalloproteinase, **TGFβ**: Transforming growth factor beta, **TIMP**: Tissue inhibitor matrix metalloproteinase

ACKNOWLEDGMENTS

None.

AUTHOR'S CONTRIBUTIONS

PDH developed the study conception and planning; ATLC, PDH, STN performed the data collection, analysis and interpretation, and statistical analysis. TML, ATLC, PDH participate effectively in research orientation. NBV, PDH, TLM participated in manuscript critical review, preparation and writing of the manuscript. PDH, NBV participated in critical literature review, approval of the final version of the manuscript. All authors read and approved the final manuscript.

FUNDING

This research is funded by Vietnam National University Ho Chi Minh City (VNU-HCM) under grant number C2023-18-18.

AVAILABILITY OF DATA AND MATERIALS

Data and materials used and/or analyzed during the current study are available from the corresponding author on reasonable request.

ETHICS APPROVAL AND CONSENT TO PARTICIPATE

Not applicable.

CONSENT FOR PUBLICATION

Not applicable.

COMPETING INTERESTS

The authors declare that they have no competing interests.

REFERENCES

1. Rong X, Chu W, Zhang H, Wang Y, Qi X, Zhang G, et al. Antler stem cell-conditioned medium stimulates regenerative wound healing in rats. Stem Cell Research & Therapy. 2019;10(1):326. PMID: 31744537. Available from: https://doi.org/10.1186/s13287-019-1457-9.
2. Xia P, Liu D, Jiao Y, Wang Z, Chen X, Zheng S. Health Effects of Peptides Extracted from Deer Antler. Nutrients. 2022;14(19):4183. PMID: 36235835. Available from: https://doi.org/10.3390/nu14194183.
3. Wang D, Berg D, Ba H, Sun H, Wang Z, Li C. Deer antler stem cells are a novel type of cells that sustain full regeneration of a mammalian organ-deer antler. Cell Death & Disease. 2019;10(6):443. PMID: 31165741. Available from: https://doi.org/10.1038/s41419-019-1686-y.
4. Seo MS, Park SB, Choi SW, Kim JJ, Kim HS, Kang KS. Isolation and characterization of antler-derived multipotent stem cells. Cell Transplantation. 2014;23(7):831–43. PMID: 23294672. Available from: https://doi.org/10.3727/096368912X661391.
5. Wang D, Berg D, Ba H, Sun H, Wang Z, Li C. Deer antler stem cells are a novel type of cells that sustain full regeneration of a mammalian organ-deer antler. Cell Death & Disease. 2019;10(6):443. PMID: 31165741. Available from: https://doi.org/10.1038/s41419-019-1686-y.
6. Li C, Yang F, Sheppard A. Adult stem cells and mammalian epimorphic regeneration-insights from studying annual renewal of deer antlers. Current Stem Cell Research & Therapy. 2009;4(3):237–51. PMID: 19492976. Available from: https://doi.org/10.2174/157488809789057446.
7. Rong X, Zhang G, Yang Y, Gao C, Chu W, Sun H. Transplanted Antler Stem Cells Stimulated Regenerative Healing of Radiation-induced Cutaneous Wounds in Rats. Cell Transplantation. 2020;29:963689720951549. PMID: 32907381. Available from: https://doi.org/10.1177/0963689720951549.
8. Yang Z, Gu L, Zhang D, Li Z, Li J, Lee M. Red Deer Antler Extract Accelerates Hair Growth by Stimulating Expression of Insulin-like Growth Factor I in Full-thickness Wound Healing Rat Model. Asian-Australasian Journal of Animal Sciences. 2012;25(5):708–16. PMID: 25049617. Available from: https://doi.org/10.5713/ajas.2011.11246.
9. Rong X, Chu W, Zhang H, Wang Y, Qi X, Zhang G, et al. Antler stem cell-conditioned medium stimulates regenerative wound healing in rats. Stem Cell Research & Therapy. 2019;10(1):326. PMID: 31744537. Available from: https://doi.org/10.1186/s13287-019-1457-9.
10. Cegielski M, Dziewiszek W, Zabel M, Dziegiel P, Kuryszko J, Izykowska I. Experimental xenoimplantation of antlerogenic cells into mandibular bone lesions in rabbits: two-year follow-up. In Vivo (Athens, Greece). 2010;24(2):165–72. PMID: 20363989.
11. Huynh PD, Tran QX, Nguyen ST, Nguyen VQ, Vu NB. Mesenchymal stem cell therapy for wound healing: an update to 2022. Biomedical Research and Therapy. 2022;9(12):5437–49. Available from: https://doi.org/10.15419/bmrat.v9i12.782.
12. Satish L, Kathju S. Cellular and Molecular Characteristics of Scarless versus Fibrotic Wound Healing. Dermatology Research and Practice. 2010;2010:790234. PMID: 21253544. Available from: https://doi.org/10.1155/2010/790234.
13. Dang CM, Beanes SR, Lee H, Zhang X, Soo C, Ting K. Scarless fetal wounds are associated with an increased matrix metalloproteinase-to-tissue-derived inhibitor of metalloproteinase ratio. Plastic and Reconstructive Surgery. 2003;111(7):2273–85. PMID: 12794470. Available from: https://doi.org/10.1097/01.PRS.0000060102.57809.DA.
14. Caley MP, Martins VL, O'Toole EA. Metalloproteinases and Wound Healing. Advances in Wound Care (New Rochelle, NY). 2015;4(4):225–34. PMID: 25945285. Available from: https://doi.org/10.1089/wound.2014.0581.
15. Monaghan M, Browne S, Schenke-Layland K, Pandit A. A collagen-based scaffold delivering exogenous microrna-29B to modulate extracellular matrix remodeling. Molecular Therapy. 2014;22(4):786–96. PMID: 24402185. Available from: https://doi.org/10.1038/mt.2013.288.
16. Zhou Y, et al. Downregulation of CFTR Is Involved in the Formation of Hypertrophic Scars. BioMed Research International. 2020;2020:9526289. Available from: https://doi.org/10.1155/2020/9526289.
17. Shah M, Foreman DM, Ferguson MW. Neutralisation of TGF-beta 1 and TGF-beta 2 or exogenous addition of TGF-beta 3 to cutaneous rat wounds reduces scarring. Journal of Cell Science. 1995;108(Pt 3):985–1002. PMID: 7542672. Available from: https://doi.org/10.1242/jcs.108.3.985.
18. Krummel TM, Michna BA, Thomas BL, Sporn MB, Nelson JM, Salzberg AM. Transforming growth factor beta (TGF-beta) induces fibrosis in a fetal wound model. Journal of Pediatric Surgery. 1988;23(7):647–52. PMID: 3204464. Available from: https://doi.org/10.1016/S0022-3468(88)80638-9.